



Synthesis, molecular docking, and biological evaluation of nitroimidazole derivatives as potent urease inhibitors

Meysam Talebi¹ · Elham Hamidian¹ · Fatemeh Niasari-Naslaji¹ · Sogand Rahmani¹ · Faezeh Sadat Hosseini¹ · Shahin Boumi¹ · Mohammad Nazari Montazer¹ · Mehdi Asadi¹ · Massoud Amanlou^{1,2}

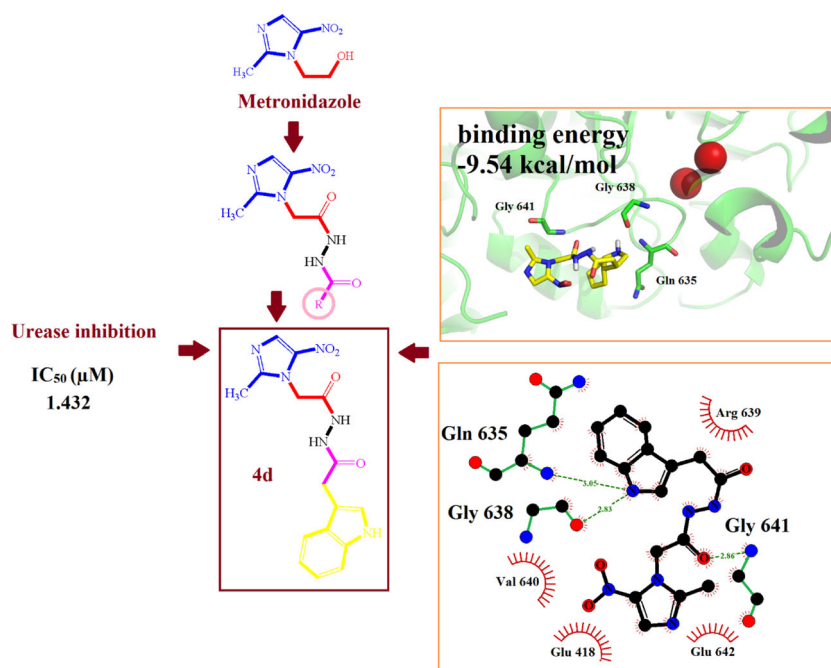
Received: 5 January 2021 / Accepted: 4 April 2021 / Published online: 12 April 2021

© The Author(s), under exclusive licence to Springer Science+Business Media, LLC, part of Springer Nature 2021

Abstract

The objective of this study was to design new nitroimidazole-based derivatives as strong urease inhibitors for the treatment of *H. pylori* infections. New series of nitroimidazole derivatives, **4a–k**, were synthesized by using TBTU as the catalyst and assayed as Jack bean urease inhibitors. The facile synthetic approach was employed for the preparation of targeted molecular designs in good to excellent yields, ranged from 65 to 92%. Accordingly, all the synthesized compounds, **4a–k** ($IC_{50} = 1.43–7.72 \mu\text{M}$), were more potent than the standard urease inhibitors, thiourea, and hydroxyurea. Among the derivatives, **4d** had the most urease inhibitor activity ($IC_{50} = 1.43 \mu\text{M}$), over 15-fold more potent than thiourea and 70-fold than hydroxyurea. True to form, the result of molecular docking studies was in good congruence with those obtained from in vitro tests.

Graphical Abstract



Supplementary information The online version contains supplementary material available at <https://doi.org/10.1007/s00044-021-02727-4>.

✉ Massoud Amanlou
amanlou@tums.ac.ir

¹ Department of Medicinal Chemistry, Faculty of Pharmacy, Tehran

University of Medical Sciences, Tehran, Iran

² Experimental Medicine Research Center, Tehran University of Medical Sciences, Tehran, Iran

Keywords Urease inhibitor · Molecular docking · Nitroimidazole · TBTU

Introduction

Helicobacter pylori (*H. pylori*) is one of the most widespread bacterial infections in the human population. However, a large number of patients do not reveal clinical pathogenic symptoms. The pathogen is transmitted orally during childhood through feces, vomitus, saliva, and water [1, 2]. *H. pylori* are well-known for triggering gastritis, gastric ulcers, and gastric adenocarcinoma [3]. Although both innate and adaptive immunity cooperate to restrain *H. pylori* from colonization, the pathogen applies various strategies to run away from the immune system [4]. *H. pylori* can exert pathogenicity by overwhelming the acidic pH of the stomach through its vital enzyme, urease, a nickel-containing enzyme that catalyzes the hydrolysis of urea to two molecules of ammonia and carbon dioxide [5–7]. It utilizes two types of urease; a surface urease, which works in neutral pH, and a cytoplasmic urease, which is activated in acidic pH (2.5–6.5). The cytoplasmic urease is responsible for bacteria's pH homeostasis. It is regulated by a H^+ -gated transporter facilitates urea permeability through the membrane and thus plays an essential role in bacterial acid resistance [8, 9].

Crystallographic analysis of *H. pylori* urease illustrates the spatial complexity of the enzyme that protects it against environmental catalytic change [10, 11]. Reports indicate that the active site of this particular enzyme in *H. pylori* is different from other bacterial ureases, which leads to a high affinity to the substrate [12]. The ammonia produced by the hydrolysis activity of urease neutralizes gastric hydrochloric acid, hence, eases bacterial colonization in epithelial cells [13].

Due to the growing concern of drug-resistant strains of *H. pylori* to antibiotics, the application of antibiotics to eliminate *H. pylori* is becoming less frequent and new methods for eradication are considered. Resistant bacteria survive from the treatment regimen, propagate, and settle in the mucosal layer of the stomach [14]. Consequently, the resistant population triggers the inoculum effect, which means a higher “minimum inhibitory concentration” is required to eradicate the pathogen

[15]. The focus is now on alternative paths, such as building an unstable acidic environment for the pathogen. Therefore, therapeutic achievements depend on abolishing the *H. pylori* urease enzyme.

A typical treatment for *H. pylori* infection involves the co-administration of a proton pump inhibitor and antibiotics [16–18]. Drug-resistant strains have been reported after the frequent use of macrolides (clarithromycin or azithromycin), tetracycline, amoxicillin, and imidazole (metronidazole or tinidazole) [19–21]. Moreover, the higher dose of these antibiotics could result in adverse effects such as nausea, vomiting, abdominal pain, diarrhea, and bloating [22–24].

Lately, the in vitro efficacy assessment of urease enzyme inhibitors using phosphoramidites has been conducted successfully [25, 26]. However, the in-vivo tests and clinical trials were not promising due to problems such as hydrolytic instability and toxicity [27, 28]. Acetohydroxamic acid is one of the few urease inhibitors that has gained FDA approval [29–31]. Nitroimidazole derivatives are commonly used in antibacterial and antiprotozoal therapies [32].

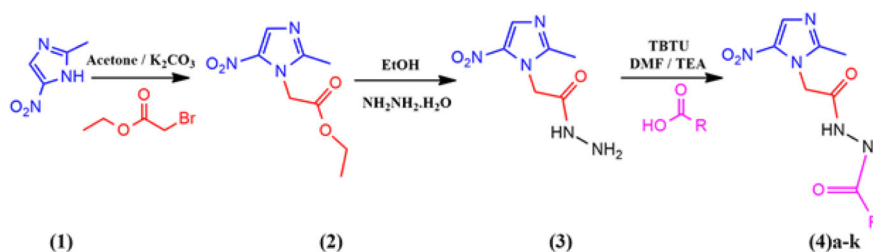
According to previous studies, a considerable number of *H. pylori* strains (6–27%) are resistant to metronidazole, a common nitroimidazole derivative [33], due to frequent medications with nitroimidazoles [34]. Then, the main objective of this study was to design new metronidazole-based derivatives with remarkable inhibitory activity that could preserve metronidazole's role as an acceptable antibiotic and could be used as strong urease inhibitors in the treatment of *H. pylori* infections.

Results and discussion

Chemistry

Eleven novel compounds have been synthesized as urease inhibitors according to the pathway shown in Scheme 1.

Scheme 1 Schematic representation of the synthesis of 2-(2-methyl-5-nitro-1H-imidazol-1-yl)acetohydrazides



Yields ranged from 65% to 92%

In this current work 2-(2-methyl-5-nitro-1H-imidazol-1-yl)acetohydrazide (**3**) was synthesized according to the previously mentioned method [35].

At the first step, ethyl 2-(2-methyl-5-nitro-1H-imidazol-1-yl)acetate (**2**) was synthesized from a reaction between 2-methyl-5-nitro-1H-imidazole (**1**) and ethyl bromoacetate in dry acetone as a solvent, then the excess amount of hydrazine hydrate was added dropwise to compound **2** in ethanol solvent to produce 2-(2-methyl-5-nitro-1H-imidazol-1-yl)acetohydrazide (**3**) [35]. In the third step, our final compounds (**4a–k**) were synthesized through a condensation reaction between 2-(2-methyl-5-nitro-1H-imidazol-1-yl)acetohydrazide (**3**) and different aromatic acid derivatives in the presence of 2-(1H-benzotriazole-1-yl)-1,1,3,3-tetramethyluronium tetrafluoroborate (TBTU) as a coupling reagent while there exist triethylamine (TEA) as base and dimethylformamide (DMF) as a solvent in our reaction medium at 0 °C. Our final compounds yield ranged from 65 to 92%. Final compound structures were confirmed by using IR and NMR spectra.

Biological activity

All eleven synthesized compounds (**4a–k**) were evaluated for their inhibitory activity against Jack bean urease. Thiourea and hydroxyurea were taken as the reference drug (Table 1). All of the tested compounds presented acceptable inhibitory activity mainly compounds **4d** ($IC_{50} = 1.43 \mu M$) and **4k** ($IC_{50} = 1.70 \mu M$). These two derivatives demonstrated potent in vitro inhibitory activity, which was comparable to standard inhibitor thiourea ($IC_{50} = 22.01 \mu M$) and hydroxyurea ($IC_{50} = 100.00 \mu M$) (Table 1). The comparison of the inhibitory activity of the synthesized compounds and metronidazole defined that the introduction of a hydrazine moiety instead of 2-hydroxy, and substitution on the benzene ring, play an important role in the urease inhibitory activity of synthetic compounds. Interestingly, methoxy-substituted compounds showed a different pattern.

Among them, compound **4k** ($IC_{50} = 1.70 \mu M$), which bears a methoxy group at ortho-position, displayed an increased inhibitory action in comparison to compounds **4c** ($IC_{50} = 4.18 \mu M$), with a methoxy group at para-position, and compound **4h** ($IC_{50} = 2.74 \mu M$), that bears both of them simultaneously.

Order of inhibitory activity stated the respective potency of **4k** > **4h** > **4c**. This outcome indicates that possibly the methoxy substitution at para-position leads to an increase in the steric hindrance or the ortho substitution interacts greatly with the active site of the enzyme. However, all of these compounds were more active as compared to the standard. Compound **4d** ($IC_{50} = 1.43 \mu M$), holding an indole-3-acetic acid moiety, displayed fifteen-fold more activity in comparison to the standard thiourea and was the

most potent derivative of the series. The desirable activity of this compound might be as a result of the appropriate binding interaction of the indole group with the active site of the enzyme. Subsequently, compound **4d** exhibited a great inhibitory activity against Jack bean urease (Table 1), which fascinated our interest in more structure modification of them as lead compounds for new urease inhibitors or anti-*H. pylori* agents.

Docking study

To predict possible interactions between the synthesized compounds and the active site of the Jack bean urease enzyme, molecular docking simulations were performed. Docking results indicate that all of the compounds interact well with the active site of the enzyme with a binding energy range of -9.54 to -6.84 kcal/mol, which are stronger than the binding energy of the standard compounds thiourea and hydroxyurea, with a binding energy of -3.45 and -5.57 kcal/mol, respectively (Table 1). The superimposed position of docking poses of all compounds in the active site of the enzyme was shown in Fig. 1a. The highest binding energy, -9.54 kcal/mol, is related to compound **4d**, representing the highest urease inhibitory activity with an IC_{50} of $1.432 \mu M$ in comparison to other compounds. The placement of the compound **4d** in the active site suggests that the inhibitory effect is probably related to the conformational changes that occur at the entrance of the tunnel leading to the nickel atoms, and therefore, it could prevent the substrate from entering the tunnel (Fig. 1b). Compound **4d**, with an indole ring, forms three hydrogen bonds with Gln 635, Gly 638, and Gly 641 residues and interacts hydrophobically with Glu 418, Arg 639, Val 640, and Glu 642 (Fig. 1c). The SwissADME webserver was used to determine the ADME properties [36]. So, compound **4d**, with a molecular weight of 356.34 g/mol, $\log p -0.14$, forms 3 and 5 hydrogen bonds, donor and acceptor, respectively, fulfill all the criteria declared in the Lipinski rule of five (Fig. 1d) and preset its potential drug ability [37]. It is expected that compound **4d**, with the highest urease inhibitory activity, and also the highest binding interactions, and proper ADME properties, could be a promising candidate for further evaluation.

Conclusion

In this current work, eleven new nitroimidazole derivatives were synthesized and their inhibitory activity against the Jack bean urease enzyme was determined. The obtained results demonstrated that all the synthesized compounds were more potent than the standard inhibitors. The docking study showed that all of the compounds successfully

Table 1 The urease inhibitory activity and docking results of compounds **4a–k**

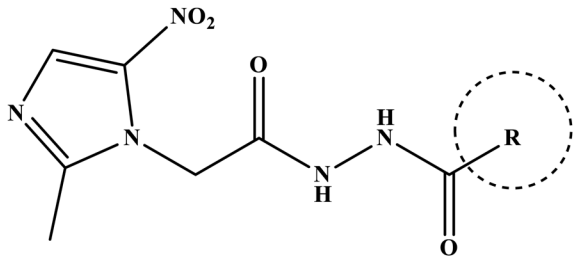
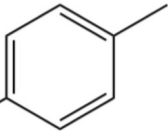
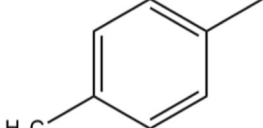
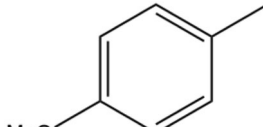
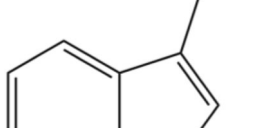
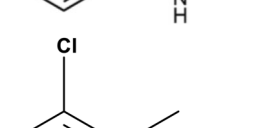
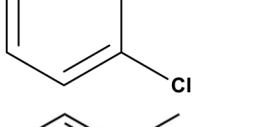
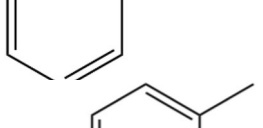
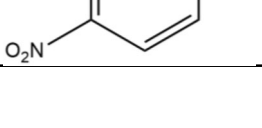
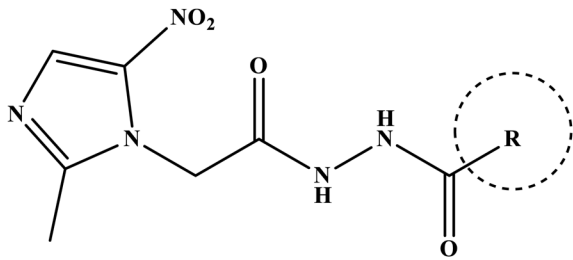
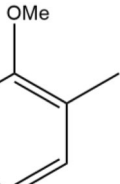
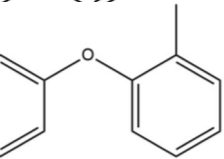
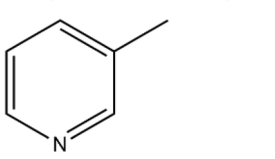
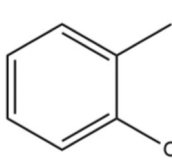
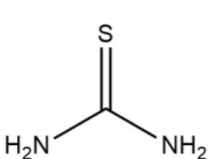
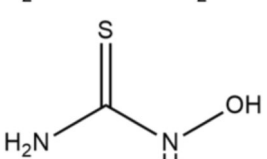
Entry	R	IC ₅₀ (μM)	ΔG binding (kcal/mol)	MW
				
4 _a		2.075	-7.67	337
4 _b		4.926	-8.17	317
4 _c		4.189	-7.73	333
4 _d		1.432	-9.54	358
4 _e		7.12	-6.99	371
4 _f		2.86	-8.03	303
4 _g		3.211	-8.56	348
				

Table 1 (continued)



Entry	R	IC ₅₀ (μM)	ΔG binding (kcal/mol)	MW
4 _h		2.747	-8.06	363
4 _i		3.786	-8.81	395
4 _j		7.724	-6.84	304
4 _k		1.702	-7.75	333
Thiourea		22.01	-3.45	76
Hydroxyurea		100.00	-5.57	76

Thiourea and hydroxyurea were used as standards urease inhibitors

occupied and interacted with the active site of the urease enzyme. Eventually, among all compounds, compound **4d** indicates the lowest IC₅₀ value of urease inhibitory activity

and lowest docking binding energy and is known as the potent compound of this series. According to the urease inhibitory activity of our final compounds, it seems

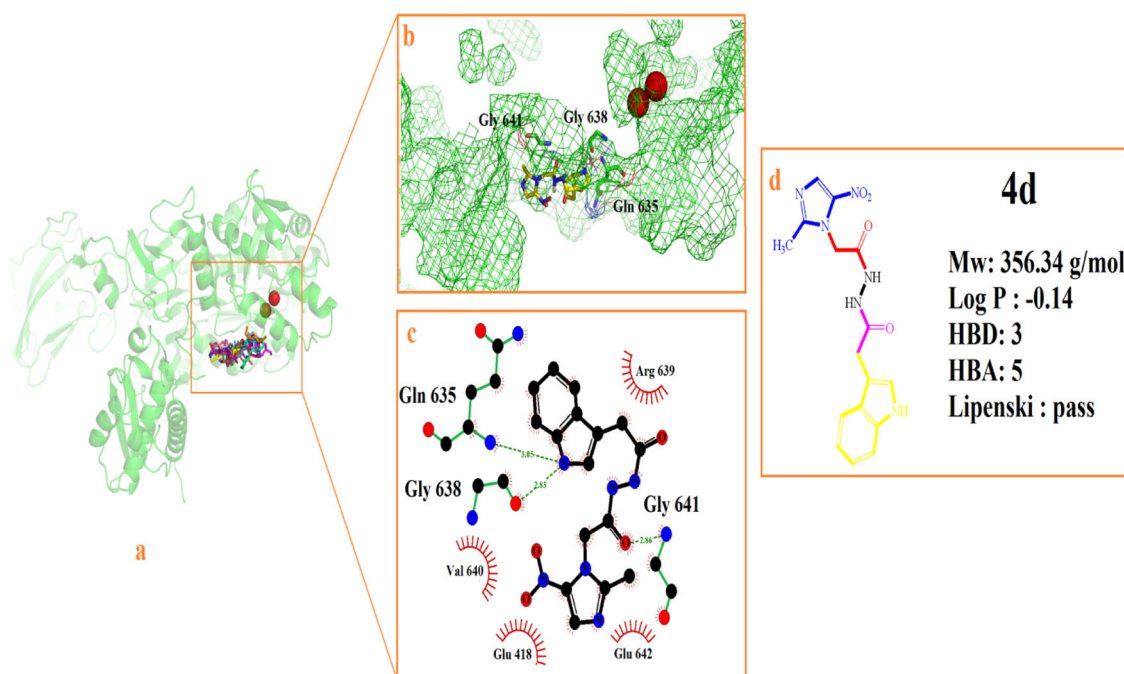


Fig. 1 **a** Superimposed of docking position of all compounds in the active site of the urease enzyme, atom Ni are in red sphere. **b**, **c** 3D and 2D display of interactions of compound **4d** in the active site of urease enzyme, **d** structure of compound **4d** and its ADME property

beneficial to consider nitroimidazole as an important moiety for design and synthesize potent urease inhibitors.

Experimental/material and methods

General

All chemicals used in this study were obtained from Merck (Germany) and used without further purification. Melting points were determined with a Kofler hot stage apparatus and were uncorrected. ^1H and ^{13}C NMR spectra were recorded with a Bruker FT-500, using TMS as an internal standard. Coupling constant (J) values are presented in Hertz (Hz), and spin multiples are given as s (singlet), d (doublet), t (triple), and m (multiple). Infrared spectra were acquired on a Nicolet Magna 550-FT spectrometer. IR spectra of solid were recorded in KBr, and the absorption band was given in wavenumbers in cm^{-1} .

Urease inhibitory activity

Sodium nitroprusside and Jack bean urease (EC 3.5.1.5) were purchased from Sigma (St. Louis, MO, USA). Ultra-pure water (HPLC grade, Duksan, Korea) was utilized in all experiments. The compounds including, **4a–k** and inhibitors, were dissolved in deionized water. The urease inhibitory activity of the synthesized compounds was assessed by a procedure explained previously [38, 39].

In brief, the modified Berthelot spectrophotometric method was used to evaluate urease inhibitory of the synthesized derivatives at the concentration range of 0–10 mg/ml and measuring the absorbance at 625 nm. The jack bean urease enzyme was activated after 30 min incubation at 37 °C, and then, the absorbance of the testing solutions was measured after adding a combination of phenol and alkali reagents. The thiourea and hydroxyurea were used as the reference standard inhibitors, and all the experiments were performed in triplicate.

Finally, the percentage of urease inhibition activity was calculated as

$$\text{Inhibition (\%)} = [1 - (T/C)] \times 100$$

T is the absorbance of the test samples (synthesized compounds (**4a–k**) or positive control) in the presence of the enzyme, and C (control) is the absorbance of the reagents in the presence of the enzyme. The IC_{50} values were calculated using GraphPad Prism 5 software (Graph-Pad Software Inc., San Diego, CA) (Table 1).

Docking method

Preparation of the input files of the ligands and receptor was done by AutoDockTools 1.5.6 (ADT) [40]. Jack bean urease enzyme with PDB ID: 3LA4 was downloaded from the protein data bank. MarvinSketch version 15.2.2 was used to draw the structure of the ligands in 2D format. Chem3D ultra version 8.0 was used to minimized energy

and converting the 2D structure to PDB format. Receptor preparation was performed as follows, all water molecules were deleted, and then polar hydrogens were added and, Kollman charges were assigned, and non-polar hydrogens were merged. Grid box with the size of $60 \times 60 \times 60 \text{ \AA}$ with grid center $-43.931, -43.497, 77.423$ (X, Y, and Z) and grid-point spacing of 0.375 \AA was located near the Ni atom in the active site of the enzyme. The grid maps of each atom type were calculated by AutoGrid 4.2 [40]. The following parameter was set to calculate docking simulations by AutoDock 4.2: 2.5×10^6 maximum number of energy evaluations with 30 run jobs and Lamarckian genetic algorithm (LGA) with the population size of 150, and the default value for the rest of the parameters [39–41]. The docking poses with the lowest binding energy value of each compound were used to illustrate by LIGPLOT⁺ version v.2.2 [42] and PyMol version 1. Level [43].

General procedure for the synthesis of compounds 4a–k

Ethyl (2-methyl-5-nitro-1H-imidazol-1-yl)acetate (2)

A mixture of 2-methyl-5-nitro-1H-imidazole **1** (1 mmol), ethyl bromoacetate (1 mmol), and potassium carbonate (1.5 mmol) (5–10 mL) was refluxed in dry acetone for 50 h. The reaction mixture was cooled to room temperature, and the solvent was distilled off from the filtrate. The crude ester thus obtained was purified by recrystallization from ethanol. Yield 85% (213.07 mg); mp $96 \text{ }^\circ\text{C}$ [35].

2-(2-methyl-5-nitro-1H-imidazol-1-yl)acetohydrazide (3)

Ethyl (2-methyl-5-nitro-1H-imidazol-1-yl)acetate **2** (2 mmol) was dissolved in ethanol as a solvent and, then, an excessive amount of hydrazine hydrate (3 mmol) was added dropwise to the mixture. The reaction mixture was refluxed for 10 h and then cooled to room temperature. The solid formed, filtered, dried, and recrystallized from ethanol to get pure compound **3**. Yield 60% (238.8 mg); mp $189 \text{ }^\circ\text{C}$ [35].

Experimental procedure for the synthesis of nitroimidazole derivatives (4a–k)

A mixture of benzoic acid derivatives (1 mmol), 0.32 g (1 mmol) of TBTU, and 0.28 mL (2 mmol) of triethylamine (TEA) in 2 mL dimethylformamide (DMF) was stirred at $0 \text{ }^\circ\text{C}$ for 3 min. Then 2-(2-methyl-5-nitro-1H-imidazol-1-yl)acetohydrazide **3** (1 mmol) was added to the reaction medium. The reaction mixture was stirred at $0 \text{ }^\circ\text{C}$ for 1 h and left overnight at room temperature. The reaction mixture was poured into ice water, filtered, washed with 5% aqueous citric acid solution ($2 \times 10 \text{ mL}$), saturated sodium

bicarbonate solution ($2 \times 10 \text{ mL}$), and water. The crude product was recrystallized from dichloromethane to obtain pure final compounds (**4a–k**).

4-chloro-N'-(2-(2-methyl-5-nitro-1H-imidazol-1-yl)acetyl) benzohydrazide (4a)

White solid; yield: 78% (263.4 mg), mp = $231\text{--}233 \text{ }^\circ\text{C}$. IR (KBr): ν_{max} 3318 (NH), 3055 (C–H aromatic), 2986 (C–H aliphatic), 1688 (C=O), 1563–1358 (NO_2) cm^{-1} . ^1H NMR (DMSO- d_6 , 500 MHz): δ = 2.34 (s, 3H, CH_3), 4.97 (s, 2H, CH_2), 7.58–7.60 (d, J = 8.1 Hz, 2H, H-3, H-5), 7.88–7.90 (d, J = 8.1 Hz, 2H, H-2, H-6), 8.35 (s, 1H, CH, Imidazole), 10.55–10.67 (m, 2H, 2 \times NH) ppm. ^{13}C NMR (DMSO- d_6 , 500 MHz): δ = 13.1 (CH_3), 48.2 (CH_2), 129.3 (C-1, Ph), 129.9 (CH, Ph), 130.2 (CH, Ph), 131.4 (CH, Ph), 137.5 (C-4, Ph), 137.8 (C-4, imidazole), 145.7 (C-5, imidazole), 146.5 (C-2, imidazole), 165.1 (C=O), 165.9 (C=O) ppm. HRMS: m/z [$\text{M} + \text{H}$]⁺ calcd for $\text{C}_{13}\text{H}_{12}\text{ClN}_5\text{O}_4$: 338.0650, found: 337.0578.

4-methyl-N'-(2-(2-methyl-5-nitro-1H-imidazol-1-yl)acetyl) benzohydrazide (4b)

White solid; yield: 78% (247.5 mg), mp = $228\text{--}230 \text{ }^\circ\text{C}$. IR (KBr): ν_{max} 3375 (NH), 3089 (C–H aromatic), 2979 (C–H aliphatic), 1680 (C=O), 1558–1346 (NO_2) cm^{-1} . ^1H NMR (DMSO- d_6 , 500 MHz): δ = 2.25 (s, 3H, CH_3), 2.36 (s, 3H, CH_3), 4.96 (s, 2H, CH_2), 7.21–7.23 (d, J = 8.25 Hz, 2H, H-3, H-5), 7.86–7.88 (d, J = 8.25 Hz, 2H, H-2, H-6), 8.35 (s, 1H, CH, Imidazole), 10.43 (s, 2H, 2 \times NH) ppm. ^{13}C NMR (DMSO- d_6 , 500 MHz): δ = 13.1 (CH_3), 21.6 (CH_3), 48.2 (CH_2), 123.9 (C-4, Ph), 128.0 (CH, Ph), 129.6 (CH, Ph), 129.7 (C–H, Ph), 129.9 (C-1, Ph), 142.6 (C-4, Imidazole), 145.7 (C-5, Imidazole), 146.5 (C-2, Imidazole), 165.9 (C=O), 166.0 (C=O) ppm. HRMS: m/z [$\text{M} + \text{H}$]⁺ calcd for $\text{C}_{14}\text{H}_{15}\text{N}_5\text{O}_4$: 317.1124, found: 318.1199.

4-methoxy-N'-(2-(2-methyl-5-nitro-1H-imidazol-1-yl)acetyl) benzohydrazide (4c)

White solid; yield: 72% (239.9 mg), mp = $249\text{--}251 \text{ }^\circ\text{C}$. IR (KBr): ν_{max} 3335 (NH), 3026 (C–H aromatic), 2991 (C–H aliphatic), 1680 (C=O), 1558–1354 (NO_2) cm^{-1} . ^1H NMR (DMSO- d_6 , 500 MHz): δ = 2.36 (s, 3H, CH_3), 4.96 (s, 2H, CH_2), 7.02–7.04 (d, J = 8.35 Hz, 2H, H-3, H-5), 7.86–7.88 (d, J = 8.35 Hz, 2H, H-2, H-6), 8.35 (s, 1H, CH, Imidazole), 10.43 (s, 2H, 2 \times NH) ppm. ^{13}C NMR (DMSO- d_6 , 500 MHz): δ = 13.1 (CH_3), 48.2 (CH_2), 56.0 (O– CH_3), 114.3 (CH-2, Ph), 114.4 (C-6, Ph), 124.0 (CH-3, Ph), 124.3 (CH-5, Ph), 124.8, 130.0 (C-1, Ph), 141.3 (C-4, Imidazole), 145.7 (C-5, Imidazole), 146.5 (C-2, Imidazole), 163.0 (C-4, Ph), 165.6 (C=O), 165.9 (C=O) ppm. HRMS: m/z [$\text{M} + \text{H}$]⁺ calcd for $\text{C}_{14}\text{H}_{15}\text{N}_5\text{O}_5$: 333.1073, found: 332.1003.

(1H-Indol-3-yl)-acetic acid N'-(2-(2-methyl-5-nitro-imidazol-1-yl)-acetyl)-hydrazide (4d)

White solid; yield: 65% (231.6 mg), mp = 234–236 °C. IR (KBr): ν_{\max} 3318 (NH), 3055 (C–H aromatic), 2986 (C–H aliphatic), 1688 (C=O), 1563–1358 (NO₂) cm⁻¹. ¹H NMR (DMSO-d₆, 500 MHz): δ = 2.29 (s, 3H, CH₃), 3.59 (s, 2H, CH₂), 4.87 (s, 2H, CH₂), 6.96–6.99 (t, *J* = 7.75 Hz, 1H, H-4), 7.05–7.08 (t, *J* = 7.75 Hz, 1H, H-5), 7.24 (d, *J* = 2.5 Hz, 1H, H-2), 7.33–7.35 (d, *J* = 8.3 Hz, 1H, H-7), 7.57–7.59 (d, *J* = 8.3 Hz, 1H, H-4), 8.31 (s, 1H, CH, Imidazole'), 10.20 (s, 1H, NH), 10.37 (s, 1H, NH), 10.89 (s, 1H, NH) ppm. ¹³C NMR (DMSO-d₆, 500 MHz): δ = 13.1 (CH₃), 31.1 (CH₂), 48.1 (CH₂), 108.6 (C-3-indole), 111.9 (CH-7-indole), 118.9 (CH-4-indole), 119.3 (CH-5-indole), 121.6 (CH-6-indole), 124.0 (CH-2-indole), 124.5 (C-3a-indole), 127.7 (C-7a-indole), 136.6 (C-4, Imidazole), 145.7 (C-5, Imidazole), 146.4 (C-2, Imidazole), 165.4 (C=O), 170.2 (C=O) ppm. HRMS: *m/z* [M+H]⁺ calcd for C₁₆H₁₆N₆O₄: 356.1233, found: 357.1307.

2,6-dichloro-N'-(2-(2-methyl-5-nitro-1H-imidazol-1-yl)acetyl)benzohydrazide (4e)

White solid; yield: 65% (241.9 mg), mp = 221–223 °C. IR (KBr): 3348 (NH), 3029 (C–H aromatic), 2964 (C–H aliphatic), 1672 (C=O), 1545–1359 (NO₂) cm⁻¹. ¹H NMR (DMSO-d₆, 500 MHz): δ = 2.34 (s, 3H, CH₃), 4.46 (s, 2H, CH₂), 7.59–7.62 (t, *J* = 7.6 Hz, 1H, H-4), 7.79–7.81 (d, *J* = 7.65 Hz, 2H, H-3, H-5), 8.25 (s, 1H, CH, Imidazole'), 10.21 (s, 2H, 2×NH) ppm. ¹³C NMR (DMSO-d₆, 500 MHz): δ = 13.4 (CH₃), 48.8 (CH₂), 126.4 (CH-4, Ph), 129.1 (CH-3, Ph), 129.6 (CH-5, Ph), 131.8 (C-2, Ph), 132.3 (C-6, Ph), 133.7 (C-4, Imidazole), 135.1 (C-5, Imidazole), 141.3 (C-2, Imidazole), 164.0 (C=O), 165.4 (C=O) ppm. HRMS: *m/z* [M+H]⁺ calcd for C₁₃H₁₂FN₅O₄: 321.0873, found: 322.0943.

N'-(2-(2-methyl-5-nitro-1H-imidazol-1-yl)acetyl)benzohydrazide (4f)

White solid; yield: 84% (254.7 mg), mp = 234–236 °C. IR (KBr): ν_{\max} 3340 (NH), 3063 (C–H aromatic), 2978 (C–H aliphatic), 1679 (C=O), 1550–1352 (NO₂) cm⁻¹. ¹H NMR (DMSO-d₆, 500 MHz): δ = 2.35 (s, 3H, CH₃), 4.97 (s, 2H, CH₂), 7.49–7.52 (t, *J* = 7.6 Hz, 2H, H-3, H-5), 7.56–7.58 (t, *J* = 7.65 Hz, 1H, H-4), 7.87 (d, *J* = 7.6 Hz, 2H, H-2, H-6), 8.34–8.36 (s, 1H, CH, Imidazole'), 10.53 (s, 2H, 2×NH) ppm. ¹³C NMR (DMSO-d₆, 500 MHz): δ = 13.1 (CH₃), 48.2 (CH₂), 124.0 (CH-4, Ph), 128.1 (CH-3, Ph), 128.2 (CH-5, Ph), 129.1 (CH-2, Ph), 129.2 (CH-6, Ph), 132.6 (C-1, Ph), 136.7 (C-4, Imidazole), 145.7 (C-5, Imidazole), 146.5 (C-2, Imidazole), 165.9 (C=O), 166.1 (C=O) ppm. HRMS:

m/z [M+H]⁺ calcd for C₁₃H₁₃N₅O₄: 303.0968, found: 304.1042.

N'-(2-(2-methyl-5-nitro-1H-imidazol-1-yl)acetyl)-4-nitrobenzohydrazide (4g)

White solid; yield: 92% (320.4 mg), mp = 272–274 °C. IR (KBr): ν_{\max} 3358 (NH), 3055 (C–H aromatic), 2983 (C–H aliphatic), 1692 (C=O), 1568–1360 (NO₂) cm⁻¹. ¹H NMR (DMSO-d₆, 500 MHz): δ = 2.35 (s, 3H, CH₃), 4.99 (s, 2H, CH₂), 8.09–8.11 (d, *J* = 8.25 Hz, 2H, H-2, H-6), 8.35 (s, 1H, CH, Imidazole), 8.36–8.38 (d, *J* = 8.25 Hz, 2H, H-3, H-5), 10.80 (s, 2H, 2×NH) ppm. ¹³C NMR (DMSO-d₆, 500 MHz): δ = 13.1 (CH₃), 48.2 (CH₂), 124.0 (C-1, Ph), 124.3 (CH-3, Ph), 124.4 (CH-2, Ph), 138.3 (C-4, Imidazole), 145.7 (C-5, Imidazole), 146.5 (C-2, Imidazole), 150.1 (C-4, Ph), 164.6 (C=O), 165.8 (C=O) ppm. HRMS: *m/z* [M+H]⁺ calcd for C₁₃H₁₂N₆O₆: 348.0818, found: 347.0743.

2,4-dimethoxy-N'-(2-(2-methyl-5-nitro-1H-imidazol-1-yl)acetyl)benzohydrazide (4h)

White solid; yield: 75% (272.4 mg), mp = 237–239 °C. IR (KBr): ν_{\max} 3328 (NH), 3040 (C–H aromatic), 2975 (C–H aliphatic), 1680 (C=O), 1555–1355 (NO₂) cm⁻¹. ¹H NMR (DMSO-d₆, 500 MHz): δ = 2.35 (s, 3H, CH₃), 3.83 (s, 3H, O–CH₃), 3.90 (s, 3H, O–CH₃), 4.92 (s, 2H, CH₂), 6.79–6.80 (d, *J* = 1.5 Hz, 2H, H-3, H-5), 7.79 (s, 1H, H-6), 8.32 (s, 1H, CH, Imidazole'), 9.88 (s, 1H, NH), 10.69 (s, 1H, NH) ppm. ¹³C NMR (DMSO-d₆, 500 MHz): δ = 13.1 (CH₃), 48.1 (CH₂), 56.1 (O–CH₃), 56.7 (O–CH₃), 99.1 (CH-2, Ph), 106.5 (CH-5, Ph), 124.0 (C-1, Ph), 133.1 (C-4, Imidazole), 145.7 (C-5, Imidazole), 146.5 (C-2, Imidazole), 159.4 (C-2, Ph), 163.8 (C-4, Ph), 164.2 (C=O), 164.8 (C=O) ppm. HRMS: *m/z* [M+H]⁺ calcd for C₁₅H₁₇N₅O₆: 363.1179, found: 364.1256.

N'-(2-(2-methyl-5-nitro-1H-imidazol-1-yl)acetyl)-2-phenoxybenzohydrazide (4i)

White solid; yield: 68% (268.8 mg), mp = 195–197 °C. IR (KBr): ν_{\max} 3346 (NH), 3052 (C–H aromatic), 2984 (C–H aliphatic), 1685 (C=O), 1548–1339 (NO₂) cm⁻¹. ¹H NMR (DMSO-d₆, 500 MHz): δ = 2.32 (s, 3H, CH₃), 4.91 (s, 2H, CH₂), 6.87–6.89 (d, *J* = 8.35 Hz, 1H, H₃), 7.05–7.07 (d, *J* = 7.9 Hz, 2H, H-2, H-6), 7.16–7.19 (t, *J* = 8.3 Hz, 1H, H-4), 7.64–7.66 (d, *J* = 7.6 Hz, 1H, H-6), 8.32 (s, 1H, CH, Imidazole'), 10.33 (s, 1H, NH), 10.65 (s, 1H, NH) ppm. ¹³C NMR (DMSO-d₆, 500 MHz): δ = 13.1 (CH₃), 48.1 (CH₂), 119.1 (CH-2',6', Ph), 119.2 (CH-4', Ph), 119.8 (CH-3, Ph), 123.9 (CH-5, Ph), 124.5 (C-1, Ph), 126.1 (CH-6, Ph), 130.6 (CH-3',5', Ph), 132.9 (C-4, Imidazole), 145.7 (C-5,

Imidazole), 146.5 (C-2, Imidazole), 154.9 (C-2, Ph), 156.7 (CH-1', Ph), 164.9 (C=O), 165.3 (C=O) ppm. HRMS: m/z $[M+H]^+$ calcd for $C_{19}H_{17}N_5O_5$: 395.1229, found: 396.1302.

N'-(2-(2-methyl-5-nitro-1H-imidazol-1-yl)acetyl)nicotinohydrazide (4j)

White solid; yield: 68% (206.9 mg), mp = 266–268 °C. IR (KBr): ν_{max} 3338 (NH), 3045 (C–H aromatic), 2988 (C–H aliphatic), 1679 (C=O), 1610 (C = N), 1564–1342 (NO_2) cm^{-1} . 1H NMR (DMSO- d_6 , 500 MHz): δ = 2.35 (s, 3H, CH_3), 4.97 (s, 2H, CH_2), 7.52–7.54 (d, J = 6.5 Hz, 1H, H_5), 8.20–8.22 (d, J = 7.7 Hz, 1H, H-6), 8.34 (s, 1H, CH, Imidazole), 8.73–8.75 (t, J = 3.5 Hz, 1H, H-5), 9.02 (s, 1H, H-2), 10.68 (s, 2H, 2 \times NH) ppm. ^{13}C NMR (DMSO- d_6 , 500 MHz): δ = 13.1 (CH_3), 48.3 (CH_2), 123.7 (C-5-pyridin), 124.3 (C-1-pyridin), 135.0 (C-6-pyridin), 135.7 (C-4, Imidazole), 145.7 (C-5, Imidazole), 146.5 (C-2, Imidazole), 149.0 (C-4-pyridin), 152.9 (C-2-pyridin), 164.4 (C=O), 165.4 (C=O) ppm. HRMS: m/z $[M+H]^+$ calcd for $C_{12}H_{12}N_6O_4$: 304.0920, found: 305.0992.

2-methoxy-N'-(2-(2-methyl-5-nitro-1H-imidazol-1-yl)acetyl)benzohydrazide (4k)

White solid; yield: 70% (231.2 mg), mp = 251–253 °C. IR (KBr): ν_{max} 3358 (NH), 3044 (C–H aromatic), 2989 (C–H aliphatic), 1680 (C=O), 1545–1360 (NO_2) cm^{-1} . 1H NMR (DMSO- d_6 , 500 MHz): δ = 2.35 (s, 3H, CH_3), 3.88 (s, 3H, O- CH_3), 4.94 (s, 2H, CH_2), 7.04–7.07 (t, J = 7.7 Hz, 1H, H-5), 7.15–7.17 (d, J = 8.35 Hz, 1H, H-3), 7.50–7.53 (t, J = 7.85 Hz, 1H, H-4), 7.71–7.73 (d, J = 7.85 Hz, 1H, H-6), 8.34 (s, 1H, CH, Imidazole), 10.10 (s, 1H, NH), 10.72 (s, 1H, NH) ppm. ^{13}C NMR (DMSO- d_6 , 500 MHz): δ = 13.1 (CH_3), 48.1 (CH_2), 56.5 (CH_3), 112.7 (CH-3, Ph), 121.2 (CH-5, Ph), 122.0 (C-1, Ph), 124.2 (CH-4, Ph), 130.9 (CH-6, Ph), 133.6 (C-4, Imidazole), 145.7 (C-5, Imidazole), 146.5 (C-2, Imidazole), 157.6 (C-2, Ph), 165.0, 165.1 (C=O), 165.5 (C=O) ppm. HRMS: m/z $[M+H]^+$ calcd for $C_{14}H_{15}N_5O_5$: 333.1073, found: 334.1146.

Acknowledgements The research reported in this publication was supported by Elite Researcher Grant Committee under award number [996450] from the National Institute for Medical Research Development (NIMAD), Tehran, Iran.

Compliance with ethical standards

Conflict of interest The authors declare no competing interest.

Publisher's note Springer Nature remains neutral with regard to jurisdictional claims in published maps and institutional affiliations.

References

1. Cave DR. Transmission and epidemiology of *Helicobacter pylori*. *Am J Med.* 1996;100:12S–8S. [https://doi.org/10.1016/S0002-9343\(96\)80224-5](https://doi.org/10.1016/S0002-9343(96)80224-5)
2. Suerbaum S, Michetti P. *Helicobacter pylori* infection. *N Engl J Med.* 2002;347:1175–86. <https://doi.org/10.1056/NEJMra020542>
3. Krzyżek P, Gościński G, Fijałkowski K, Migdał P, Dziadas M, Owczarek A, et al. Potential of bacterial cellulose chemisorbed with anti-metabolites, 3-bromopyruvate or sertraline, to fight against *Helicobacter pylori* lawn biofilm. *Int J Mol Sci.* 2020;21:9507 <https://doi.org/10.3390/ijms21249507>
4. Portal-Celhay C, Perez-Perez GI. Immune responses to *Helicobacter pylori* colonization: mechanisms and clinical outcomes. *Clin Sci.* 2006;110:305–14. <https://doi.org/10.1042/CS20050232>
5. Svane S, Sigurdarson JJ, Finkenwirth F, Eitinger T, Karring H. Inhibition of urease activity by different compounds provides insight into the modulation and association of bacterial nickel import and ureolysis. *Sci Rep.* 2020;10:1–4. <https://doi.org/10.1021/ac60252a045>
6. Kafarski P, Talma M. Recent advances in design of new urease inhibitors: A review. *J Adv Res.* 2018;13:101–12. <https://doi.org/10.1016/j.jare.2018.01.007>
7. Mazzei L, Musiani F, Ciurli S. The structure-based reaction mechanism of urease, a nickel dependent enzyme: tale of a long debate. *J Bio Inorg Chem.* 2020;18:1–7. <https://doi.org/10.1007/s00775-021-01855-x>
8. Graham DY, Miftahussurur M. *Helicobacter pylori* urease for diagnosis of *Helicobacter pylori* infection: a mini review. *J Adv Res.* 2018;13:51–7. <https://doi.org/10.1016/j.jare.2018.01.006>
9. Hassan ST, Šudomová M. The development of urease inhibitors: what opportunities exist for better treatment of *Helicobacter pylori* infection in children? *Children.* 2017;4(1):2 <https://doi.org/10.3390/children4010002>
10. Hu LT, Foxall PA, Russell R, Mobley H. Purification of recombinant *Helicobacter pylori* urease apoenzyme encoded by ureA and ureB. *Infect Immun.* 1992;60:2657–66. PubMed:1612736
11. Zemer B. Recent advances in the chemistry of an old enzyme, urease. *Bioorg Chem.* 1991;19:116–31. [https://doi.org/10.1016/0045-2068\(91\)90048-T](https://doi.org/10.1016/0045-2068(91)90048-T)
12. Rektorschek M, Buhmann A, Weeks D, Schwan D, Bensch KW, Eskandari S, et al. Acid resistance of *Helicobacter pylori* depends on the UreI membrane protein and an inner membrane proton barrier. *Mol Microbiol.* 2000;36:141–52. <https://doi.org/10.1046/j.1365-2958.2000.01835.x>
13. Arora R, Issar U, Kakkar R. Identification of novel urease inhibitors: pharmacophore modeling, virtual screening and molecular docking studies. *J Biomol Struct Dyn.* 2019;37:4312–26. <https://doi.org/10.1080/07391102.2018.1546620>
14. Schmalstig AA, Benoit SL, Misra SK, Sharp JS, Maier RJ. Noncatalytic antioxidant role for *Helicobacter pylori* urease. *J Bacteriol.* 2018;200(17):e00124–18. <https://doi.org/10.1128/JB.00124-18>
15. Graham DY. Antibiotic resistance in *Helicobacter pylori*: implications for therapy. *Gastroenterology.* 1998;115:1272–7. [https://doi.org/10.1016/S0016-5085\(98\)70100-3](https://doi.org/10.1016/S0016-5085(98)70100-3)
16. Savarino V, Dulbecco P, De Bortoli N, Ottonello A, Savarino E. The appropriate use of proton pump inhibitors (PPIs): need for a reappraisal. *Eur. J. Intern. Med.* 2017;37:19–24. <https://doi.org/10.1016/j.ejim.2016.10.007>
17. Chen P, Li L, Wang H, Zhao J, Cheng Y, Xie J, et al. Omeprazole, an inhibitor of proton pump, suppresses De novo lipogenesis in gastric epithelial cells. *Biomed Pharmacother.* 2020;130:110472 <https://doi.org/10.1016/j.biopha.2020.110472>

18. Hassan S, Majerová M, Šudomová M, Berchová K. Antibacterial activity of natural compounds-essential oils. *Ceska Slov Farm.* 2015;64(Dec):243–53. (6)Czech. PMID: 26841699
19. Shmueli H, Topaz S, Berdinstein R, Yahav J, Melzer E. High metronidazole and clarithromycin resistance of helicobacter pylori isolated from previously treated and naïve patients. *Isr Med Assoc J.* 2020;22:562–6. PMID: 33070487
20. Gehlot V, Mahant S, Mukhopadhyay AK, Das K, De R, Kar P, et al. Antimicrobial susceptibility profiles of Helicobacter pylori isolated from patients in North India. *J Glob Antimicrob Resist.* 2016;5:51–6. PMID: 28224028
21. Chaabane NB, Al-Adhba HS. Ciprofloxacin-containing versus clarithromycin-containing sequential therapy for Helicobacter pylori eradication: A randomized trial. *Indian J Gastroenterol.* 2015;34:68–72. <https://doi.org/10.1007/s12664-015-0535-x>
22. Bartnik W. Clinical aspects of Helicobacter pylori infection. *Pol Arch Med Wewn.* 2008;118:426–30. PMID: 18714738
23. Wang Y, Zhao R, Wang B, Zhao Q, Li Z, Zhu-Ge L, et al. Sequential versus concomitant therapy for treatment of Helicobacter pylori infection: an updated systematic review and meta-analysis. *Eur J Clin Pharmacol.* 2018;74:1–13. <https://doi.org/10.1007/s00228-017-2347-7>
24. Hassan ST, Berchová K, Majerová M, Pokorná M, Švajdlenka E. In vitro synergistic effect of Hibiscus sabdariffa aqueous extract in combination with standard antibiotics against Helicobacter pylori clinical isolates. *Pharm Biol.* 2016;54:1736–40. <https://doi.org/10.3109/13880209.2015.1126618>
25. Hassan ST, Žemlička M. Plant-derived urease inhibitors as alternative chemotherapeutic agents. *Arch Pharm.* 2016;349:507–22. <https://doi.org/10.1002/ardp.201500019>
26. Kosikowska P, Berlicki L. Urease inhibitors as potential drugs for gastric and urinary tract infections: a patent review. *Expert Opin Ther Pat.* 2011;21:945–57. <https://doi.org/10.1517/13543776.2011.574615>
27. Modolo LV, de Souza AX, Horta LP, Araujo DP, de Fatima A. An overview on the potential of natural products as ureases inhibitors: A review. *J Adv Res.* 2015;6:35–44. <https://doi.org/10.1016/j.jare.2014.09.001>
28. Follmer C. Ureases as a target for the treatment of gastric and urinary infections. *J Clin Pathol.* 2010;63:424–30. <https://doi.org/10.1136/jcp.2009.072595>
29. Jain SK, Haider T, Kumar A, Jain A. Lectin-conjugated clarithromycin and acetohydroxamic acid-loaded PLGA nanoparticles: a novel approach for effective treatment of H. pylori. *AAPS PharmSciTech.* 2016;17:1131–40. <https://doi.org/10.1208/s12249-015-0443-5>
30. Umamaheshwari R, Jain N. Receptor-mediated targeting of lipobeads bearing acetohydroxamic acid for eradication of Helicobacter pylori. *J control Release.* 2004;99:27–40. <https://doi.org/10.1016/j.jconrel.2004.06.006>
31. Griffith DP. Urease stones. *Urol Res.* 1979;7:215–21. <https://doi.org/10.1007/BF00257208>
32. Naureen S, Chaudhry F, Asif N, Munawar MA, Ashraf M, Nasim FH, et al. Discovery of indole-based tetraarylimidazoles as potent inhibitors of urease with low antilipoxygenase activity. *Eur J Med Chem.* 2015;102:464–70. <https://doi.org/10.1016/j.ejmech.2015.08.011>
33. Cunha ES, Chen X, Sanz-Gaitero M, Mills DJ, Luecke H. Cryo-EM structure of Helicobacter pylori urease with an inhibitor in the active site at 2.0 Å resolution. *Nat. Commun.* 2021;12:1–8. <https://doi.org/10.1038/s41467-020-20485-6>
34. Der Wouden V, Zwet V. Nitroimidazole resistance in Helicobacter pylori. *Aliment Pharmacol Ther.* 2000;14:7–14. <https://doi.org/10.1046/j.1365-2036.2000.00675.x>
35. Wani MY, Bhat AR, Azam A, Athar F. Nitroimidazolyl hydrazones are better amoebicides than their cyclized 1, 3, 4-oxadiazoline analogues: In vitro studies and Lipophilic efficiency analysis. *Eur J Med Chem.* 2013;64:190–9. <https://doi.org/10.1016/j.ejmech.2013.03.034>
36. Daina A, Michielin O, Zoete V. SwissADME: a free web tool to evaluate pharmacokinetics, drug-likeness and medicinal chemistry friendliness of small molecules. *Sci Rep.* 2017;7:42717 <https://doi.org/10.1038/srep42717>
37. Benet LZ, Hosey CM, Ursu O, Oprea TI. BDDCS, the rule of 5 and drugability. *Adv Drug Deliv Rev.* 2016;101:89–98. <https://doi.org/10.1016/j.addr.2016.05.007>
38. Peytam F, Adib M, Mahernia S, Rahmanian-Jazi M, Jahani M, Masoudi B, et al. Isoindolin-1-one derivatives as urease inhibitors: Design, synthesis, biological evaluation, molecular docking and in-silico ADME evaluation. *Bioorg Chem.* 2019;87:1–11. <https://doi.org/10.1016/j.bioorg.2019.02.051>
39. Azizian H, Nabati F, Sharifi A, Siavoshi F, Mahdavi M, Amanlou M. Large-scale virtual screening for the identification of new Helicobacter pylori urease inhibitor scaffolds. *J Mol Model.* 2012;18:2917–27. <https://doi.org/10.1007/s00894-011-1310-2>
40. Morris GM, Huey R, Lindstrom W, Sanner MF, Belew RK, Goodsell DS, et al. AutoDock4 and AutoDockTools4: automated docking with selective receptor flexibility. *J Comput Chem.* 2009;30:2785–91. <https://doi.org/10.1002/jcc.21256>
41. Hosseini FS, Amanlou M. Anti-HCV and anti-malaria agent, potential candidates to repurpose for coronavirus infection: Virtual screening, molecular docking, and molecular dynamics simulation study. *Life Sci.* 2020;258:118205 <https://doi.org/10.1016/j.lfs.2020.118205>
42. Laskowski RA, Swindells MB. LigPlot+: multiple ligand–protein interaction diagrams for drug discovery. *J Chem Inf Model.* 2011;51:2778–86. <https://doi.org/10.1021/ci200227u>
43. Schrödinger LLC. The PyMol molecular graphics system. 2017. Available from: <https://pymol.org>